Available Online at http://www.journalajst.com

ASIAN JOURNAL OF SCIENCE AND TECHNOLOGY

ISSN: 0976-3376

Asian Journal of Science and Technology
Vol. 16, Issue, 03, pp. 13599-13610, March, 2025

RESEARCH ARTICLE

IN SILICO STUDIES OF PROTEINS INVOLVED IN MESOTHELIOMA: KEY PROTEIN INTERACTIONS OF BCL-2A1, BCL2-L-10-2, NPM2, AND CLDN-4

Ishi Bhargavi G[1*], Tenali Shouni Niveditha[2], Deepa Switha Vishnubhotla[2], Shruti Joshi[2] and Mini Fernandez[2*]

[1]Student, Department of Biotechnology, St. Francis College for Women, Hyderabad, India
[2]Faculty, Department of Biotechnology, St. Francis College for Women, Hyderabad, India

ARTICLE INFO

Article History:
Received 19th January, 2025
Received in revised form
27th January, 2025
Accepted 14th February, 2025
Published online 30th March, 2025

Keywords:
Mesothelioma, apoptotic resistance, Bcl-2A1, Bcl2-L-10-2, NPM2, CLDN-4, biomarkers, therapeutic targets, in silico analysis, homology modeling, Modeller 10.4, SAVES v6.0, ProSA, CASTp, molecular docking, Alimta, Bevacizumab, drug-protein interaction, binding pockets, targeted therapy.

ABSTRACT

Mesothelioma, a malignant cancer affecting the pleura, peritoneum, and other organs, remains a major health challenge due to its poor prognosis. Proteins like Bcl-2A1 and Bcl2-L-10-2 contribute to apoptotic resistance, while NPM2 and CLDN-4 serve as potential biomarkers and therapeutic targets. This study used in silico methods to analyze these proteins, aiming to uncover molecular insights for targeted treatments. Using FASTA sequences from NCBI and PDB, 3D models were developed via homology modeling with Modeller 10.4 and validated using SAVES v6.0 and ProSA. Active site predictions with CASTp revealed five potential binding pockets per protein. Docking studies with Alimta and Bevacizumab identified key amino acids involved in drug interactions: LEU105, GLN23, and PHE43 in Bcl-2A1; ARG38, GLY23, and TYR17 in Bcl2-L-10-2; ARG12, TRP15, and GLY30 in NPM2; and VAL132, GLY163, and LEU73 in CLDN-4. These findings highlight crucial molecular targets, offering insights for developing more effective mesothelioma therapies.

Citation: ***Ishi Bhargavi et al.*** **2025.** "In silico studies of proteins involved in Mesothelioma: Key Protein Interactions of bcl-2a1, bcl2-l-10-2, npm2, and cldn-4", *Asian Journal of Science and Technology*, 16, (03), 13599-13610.

INTRODUCTION

Mesothelioma is a cancer originating from the mesothelium, a protective layer covering internal organs, most commonly affecting the lungs' pleura, but also found in the abdomen, heart, and testicles (Mott, 2012). The disease's primary cause is asbestos exposure, a mineral once widely used for its heat resistance, now known to induce mesothelioma after a latency period of around 40 years. Symptoms include shortness of breath, swollen abdomen, chest pain, and weight loss, with over 80% of cases linked to asbestos (Robinson *et al*., 2005). The history of mesothelioma aligns with the recognition of asbestos's carcinogenic effects, beginning with early cases in the 1920s and evolving through increased awareness and regulation in the 1960s and 70s (McDonald & McDonald, 1996; Zellos & Christiani, 2004). While asbestos use has declined in many regions, its historical prevalence continues to contribute to ongoing cases (Huang *et al*., 2023). Mesothelioma types are categorized by location—pleural (80-90% of cases), peritoneal (10-15%), pericardial (less than 1%), and testicular (less than 1%)—and cell type—epithelioid (50-70% of cases), sarcomatoid (10-20%), and biphasic (20%) (Molinari n.d.; Katy Moncivais, n.d.). Pathophysiologically, asbestos exposure triggers inflammation and genetic damage in mesothelial cells through mechanisms involving TNF-α and NF-κB pathways, leading to continuous cell proliferation and cancer development (Carbone1, 2009).

Corresponding Author: Mini Fernandez
Faculty, Department of Biotechnology, St. Francis College for Women, Hyderabad, India

Mesothelioma is an aggressive form of cancer that develops in the mesothelium, the protective lining of internal organs. It most commonly affects the lungs (pleural mesothelioma) but can also occur in the abdomen (peritoneal mesothelioma), the heart (pericardial mesothelioma), or the testicles (testicular mesothelioma). Symptoms differ depending on the type: pleural mesothelioma often causes a persistent cough, chest discomfort, and difficulty breathing; peritoneal mesothelioma may result in abdominal pain, nausea, and swelling; pericardial mesothelioma can lead to chest pain and fluid buildup around the heart; while testicular mesothelioma may present with scrotal swelling or hydrocele. Early diagnosis is challenging due to the disease's subtle initial symptoms and the long latency period between exposure to asbestos and the appearance of symptoms. (Anon., n.d.). The diagnosis often relies on a combination of imaging methods such as, X-rays identify effusions and masses; CT scans provide detailed tumor localization; MRIs offer superior soft tissue contrast; and PET scans assess metabolic activity to detect metastases. A definitive diagnosis is usually made through a thoracoscopic biopsy, a minimally invasive procedure that involves inserting a camera and biopsy tools into the chest cavity to obtain tissue samples (Andrea Bianco, 2018). Given its aggressive nature, mesothelioma is predominantly diagnosed at an advanced stage, making a complete cure challenging. Treatment strategies usually include a multimodal approach—surgery, chemotherapy, and radiation therapy—tailored to the disease's stage, patient health, and tumor extent. Emerging treatments, particularly in immunotherapy, show promise in targeting cancer cells more precisely based on individual tumor characteristics. Claudin-4 (CLDN4) plays a

significant role in cancer progression, including mesothelioma. It is involved in forming tight junctions (TJs) that regulate cell-cell adhesion and barrier function. Overexpression of CLDN4 in various cancers contributes to tumor progression by affecting the tumor microenvironment, inhibiting immune cell infiltration, and limiting drug penetration, thus contributing to drug resistance. CLDN4's non-TJ functions, such as interacting with integrin β1 and YAP, promote tumor cell proliferation and epithelial-mesenchymal transition (EMT). Targeting CLDN4 with molecular therapies like anti-CLDN4 antibodies shows potential for improving cancer treatment (Rina Fujiwara-Tani, 2023). The Bcl-2 family of proteins, including Bcl-2-related protein A1 (Bcl-2A1), plays a vital role in regulating apoptosis and contributes to cancer progression and resistance to therapy. Bcl-2A1, related to other Bcl-2 proteins, contributes to chemoresistance by inhibiting apoptosis, a common issue in cancer treatment. It functions through mitochondrial pathways to prevent cytochrome C release and caspase activation. Overexpression or dysregulation of Bcl-2 family members often leads to chemotherapy resistance, impairing drug-induced apoptosis (Santanu Maji, 2018). Nucleoplasmin-2 (NPM2), particularly its isoform 2, is implicated in cancer progression, including mesothelioma. Through its interaction with histones, NPM2 is involved in chromatin regulation and gene transcription. High NPM2 expression in tumors is associated with poorer survival outcomes, suggesting its potential as a prognostic marker. NPM2 may facilitate histone deacetylation, impacting gene expression related to tumor suppression and contributing to cancer progression (Wu, 2022). Bcl2-like protein 10 (Bcl2-L-10), an isoform of the Bcl-2 family, lacks the BH3 domain but contains BH4, BH1, and BH2 domains. It inhibits apoptosis by preventing cytochrome C release and mitochondrial membrane collapse, distinct from traditional Bcl-2 proteins. Bcl2-L-10's role is specific to blocking apoptosis through the mitochondrial pathway, without affecting death receptor-mediated apoptosis (Hong Zhang, 2001). This specificity highlights its potential as a target for cancer therapies aiming to manipulate apoptotic pathways.

MATERIALS AND METHODS

Homology modelling: The target and template proteins were chosen using biological databases, including NCBI, BLAST, PDB, and ExPASy. Selection criteria included proteins with fewer than 250 amino acids, those that had been reviewed, and those with relevant publications.

Model Generation and validation: Model generation and validation were performed using several tools: SWISS-MODEL, an automatedplatform for constructing comparative models of 3D protein structures; Discovery Studio, a software suite developed by Dassault Systèmes BIOVIA for simulating small molecules and macromolecules; SAVES v6.0, a comprehensive toolkit featuring ERRAT, VERIFY3D, PROVE, PROCHECK, and WHAT CHECK for evaluating various stereochemical parameters of protein structures; and PROSA, an interactive tool designed to detect errors in 3D protein structures.

Active site prediction: The active sites of the generated models were predicted using CASTp, an online platform that provides tools for identifying, defining, and analyzing the geometric and topological properties of protein structures.

Selection of Ligands: Ligands for molecular docking were chosen from PubChem, a public database providing data on chemical compounds and their biological interactions, developed as part of the US National Institutes of Health (NIH) Molecular Libraries Roadmap Initiatives. The selected ligands included Alimta and Bevacizumab.

Docking of Ligand and Macromolecule: Docking was carried out using PyRx, a virtual screening tool for docking small-molecule libraries to macromolecules and identifying lead compounds with desired biological functions. Autodock Vina was employed through the command prompt to split the ligands, while BIOVIA Discovery Studio Visualizer was used to visualize the interactions between the ligands and the protein.

RESULTS AND DISCUSSION

Homology modelling: Selection of target protein: The accession codes "NP_001296.1", "NP_004040.1","NP_001273610.1", and "NP_065129.1" were obtained from NCBI to retrieve the FASTA sequences of Claudin-4, Bcl-2-related protein A1, Nucleoplasmin-2 isoform 2, and Bcl-2-like protein 10 isoform 2 from UniProtKB/Swiss-Prot. NCBI provides genomic data, while ExPASy, hosted by the Swiss Institute of Bioinformatics, offers protein analysis tools. The FASTA sequences will be used for homology modeling to generate 3D models of the target proteins, aiding structural and functional studies (Consortium, 2023).

Selection of template protein: A BLAST search using the FASTA sequence identified Homo sapiens proteins with query coverage over 80% and identity above 27%. Protein accession codes 6RJP_A, 4B4S_A, 3T30_A, and 7TDM_A were entered into RCSB PDB to assess unmodeled regions, and those with minimal unmodeled regions were selected. These proteins, with 85%-100% query coverage and 100% identity, were used as templates for Claudin-4, Bcl-2-related protein A1, Nucleoplasmin-2 isoform 2, and Bcl-2-like protein 10 isoform 2 (Altschul *et al*., 1990; Newell *et al*., 2013). The selected template proteins include Bfl-1 in complex with an alpha-helical peptide, which has 85% query coverage and 100% identity with a small unmodeled region. The Bcl-2: Bim BH3 complex shows 100% query coverage and identity with minimal unmodeled regions. Human nucleoplasmin (Npm2), a histone chaperone in oocytes and early embryos, also has 100% query coverage and identity but displays some unmodeled regions at three positions. Lastly, the CryoEM structure of the sFab COP-2 complex with claudin-4 has 100% query coverage and identity with a very small unmodeled region.

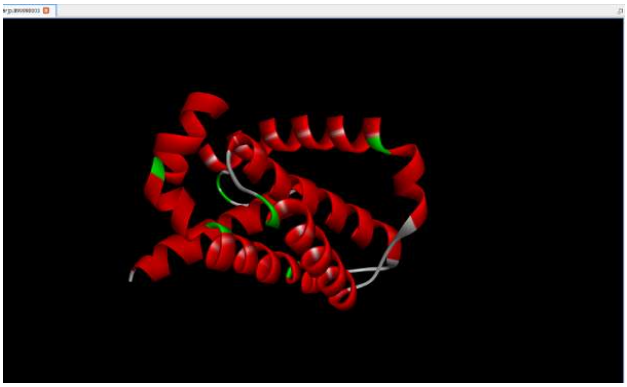

Figure 1(a). Structure of Bcl-2-related protein A1 2 generated by homology modeling

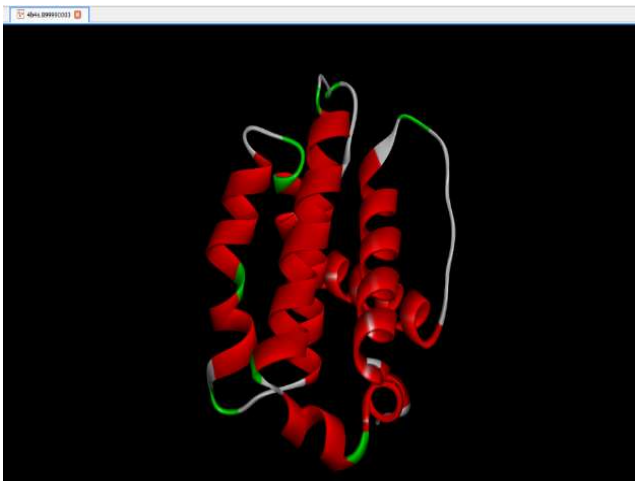

Figure 1(b): Structure of Bcl-2-like protein 10 isoform generated by homology modeling

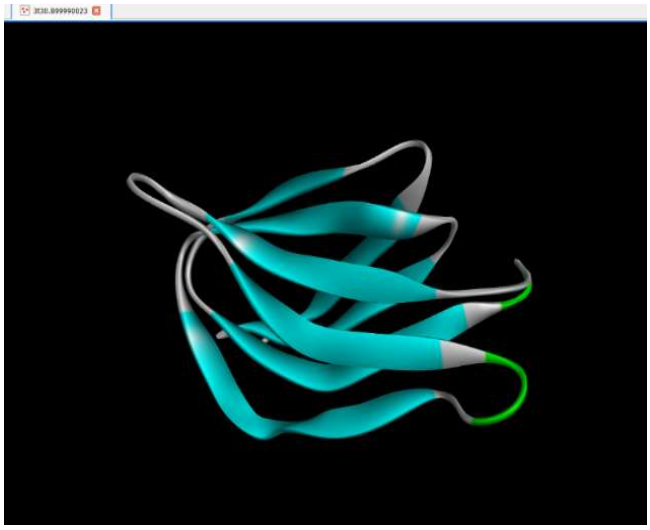

Figure 1(c). Structure of Nucleoplasmin-2-isoform homology modelling

Figure 1(d): Structure of Claudin-4 generated by generated by homology modeling

Multiple sequence alignment: A sequence alignment was performed using Clustal Omega by pasting the FASTA sequences of the target and template proteins. Clustal Omega is an automated multiple-sequence alignment tool that efficiently aligns two or more sequences (Madeira *et al*., 2022). The alignment file was generated in Pearson/FASTA and Clustal W formats, with the character count format selected as the output.

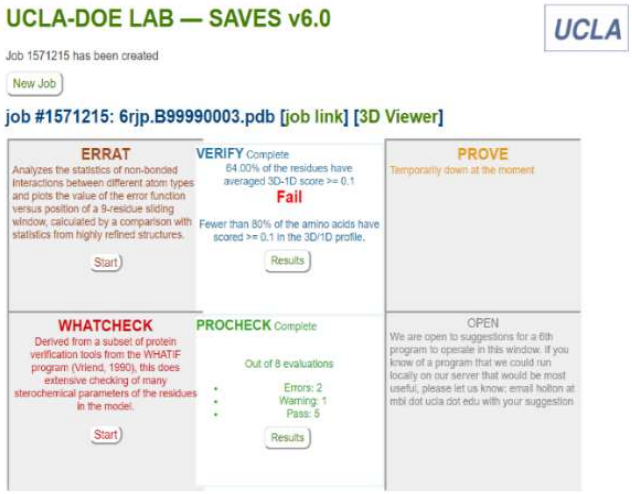

(a)

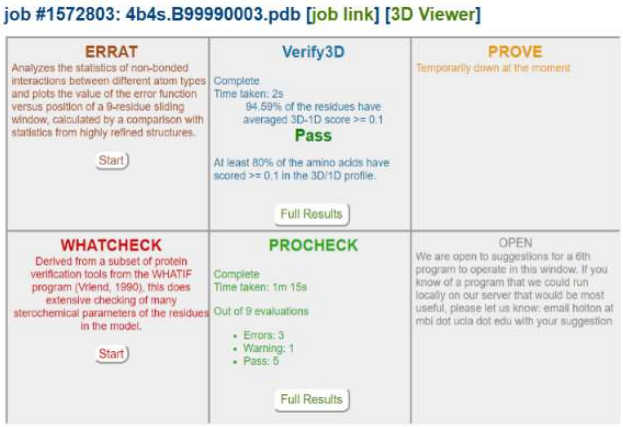

(b)

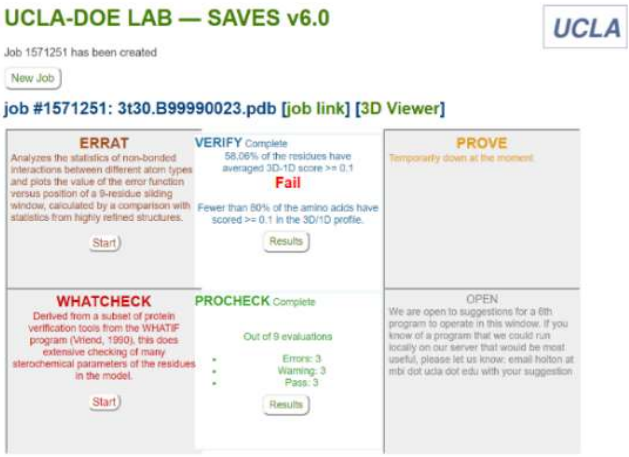

(c)

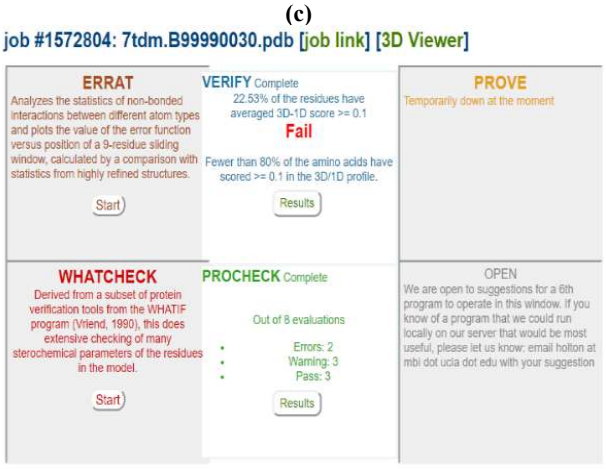

(d)

Figure 2(a),(b),(c),(d): Results of model validation From SAVES v6.0

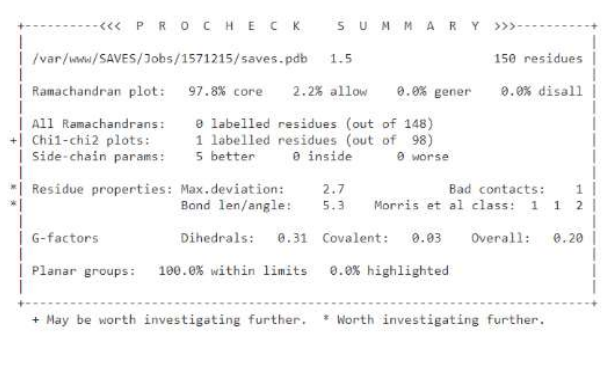

a

Summary file

b

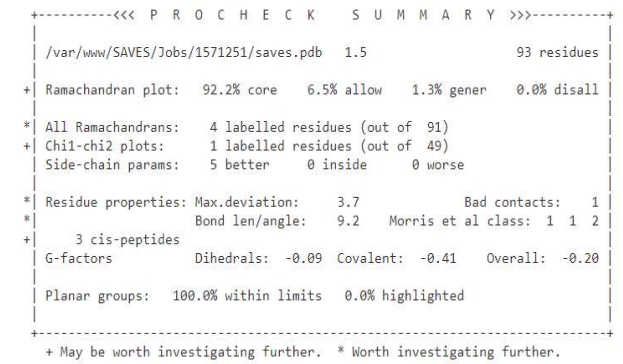

Summary file

c

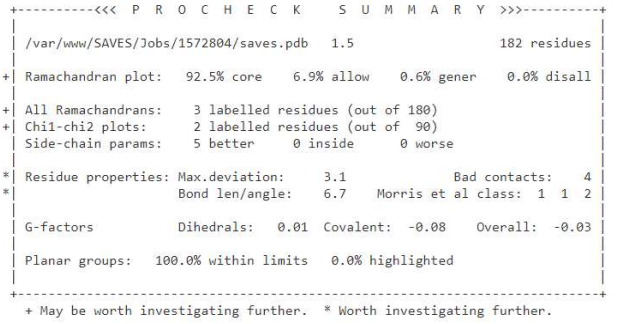

Summary file

d

Figure 3(a),(b),(c),(d). Result summaries of PROCHECK

Model Generation: The alignment.ali and model-default.py files necessary for a model generation were created by modifying the code to include data for the selected target and template proteins. Using Modeller 10.4 software, the alignment was performed, and models in PDB format were generated.Modeller, a software tool used for comparative modeling of protein structures, uses simple alignment files to calculate models containing all non-hydrogen atoms, employing the PIR format for sequence reading and writing. The generated models were assessed, and the one with the least objective function was selected. Visualization of the best model was conducted in Discovery Studio (BIOVIA, 2021). Model Validation: Model validation is done using Saves 6.0 and the following results are obtained in Verify 3D (Fig 4.16) and ProCheck (Fig 4.17). The Ramachandran plots having 97.8%, 92.2%, 95.9% & 92.5% residues in the favored region are also downloaded (Fig 4.18)

Verify 3D is a method used to assess the quality of a protein model. A model is considered of good quality if over 80% of its amino acids achieve a score of ≥0.2 in the 3D/1D profile. However, Verify 3D alone is insufficient for comprehensive validation; other parameters must also be examined. The model failed the Verify 3D assessment (Fig. 4.16), but further evaluation using Procheck (Laskowski R A, 1993) analyzed additional parameters.Since each model has over 90% residues in the highly favoured region, in the Ramachandran plotthey are valid for further studies.Further model validation was performed using ProSA web, which shows the graphs below. Figure 1.9 shows the graphs of overall model quality specifying the Z score and Figure 4.20 local model quality. The ProSA program (Sippl, 2007) is a widely used tool for refining and validating experimental protein structures using atomic coordinates in PDB format. The "Overall Model Quality" graphs display z-scores, indicating overall model quality, with X-ray crystallography (light blue) and NMR spectroscopy (dark blue) z-scores plotted against protein length. The z-scores for Bcl-2-related protein A1, Nucleoplasmin-2 isoform 2, Bcl-2-like protein 10 isoform 2, and Claudin-4 are -6.83, -6.64, -3.76, and -2.59, respectively. "Local Model Quality" energy plots show residue energies across the amino acid sequence, with positive values suggesting problematic regions. Bcl-2-related protein A1, Nucleoplasmin-2 isoform 2, and Bcl-2-like protein 10 isoform 2 have only negative values, while Claudin-4 shows mostly negative values with a few peaks. The models are validated by their negative z-scores and predominantly negative energy plots.

Active-site prediction: CASTp is used to visualize and tabulate protein pockets. The Computed Atlas of Surface Topography of Proteins (CASTp) server provides information about a protein's topographic features, identifying channels, pockets, and cavities. A cavity is an inner space inaccessible to solvent, while pockets are surface concavities where the solvent can enter, potentially serving as active sites or receptor interaction points. Protein structures in PDB format and a probe radius (default 1.4 Å) are inputs to CASTp, which predicts the active sites based on these features. The Computed Atlas of Surface Topography of Proteins (CASTp) server provides insights into the topographic features of proteins, identifying cavities, pockets, and channels within protein structures (al, 2018). Cavities are interior voids inaccessible to the solvent, while pockets are surface concavities accessible to the solvent, potentially serving as active sites (Vadija *et al*., 2016). Using protein structures in PDB format and a probe radius (default 1.4 Å), CASTp outputs details on surface pockets and cavities, including volumes, areas, and constituent atoms. Active site residues and cavity volumes for Bcl-2-related protein A1, Nucleoplasmin-2 isoform 2, Bcl-2-like protein 10 isoform 2, and Claudin-4 were predicted and tabulated based on pocket evaluation with CASTp.

Selection of Ligands: Alimta and Bevacizumab are drugs used in the treatment of the cancer Mesothelioma. The 3D conformations of the drugs were downloaded from PubChem,a public database providing information on chemical substances and their biological activities, initiated in 2004 as a part of the US National Institutes of Health (NIH) Molecular Libraries Roadmap Initiatives(Kim, 2023). The drugs were downloaded in the sdf format and further converted to the PDB format to perform docking and study the interactions between each drug (acting as a ligand) and the proteins.

Docking of ligand and macromolecule: Docking of ligands and macromolecule (protein) was performed using PyRx. A grid was formed surrounding the entire structure and Vina was run to give the results in the form of a table containing the ligand's bond affinity and rmsd values. PyRx is a software used for docking studies. The drugs (downloaded in step) are docked as ligands and the protein (target) is docked as the macromolecule. Using Vina Wizard, a Grid of suitable dimensions with respective suitable centers is generated enclosing the entire protein containing the active sites. (Vadija *et al*., 2016) Upon further running the program, a table is obtained containing the ligands, their binding affinities, and rmsd values. Rmsd refers to the root mean square deviation values and only those proteins containing 0 as rmsd values must be considered.

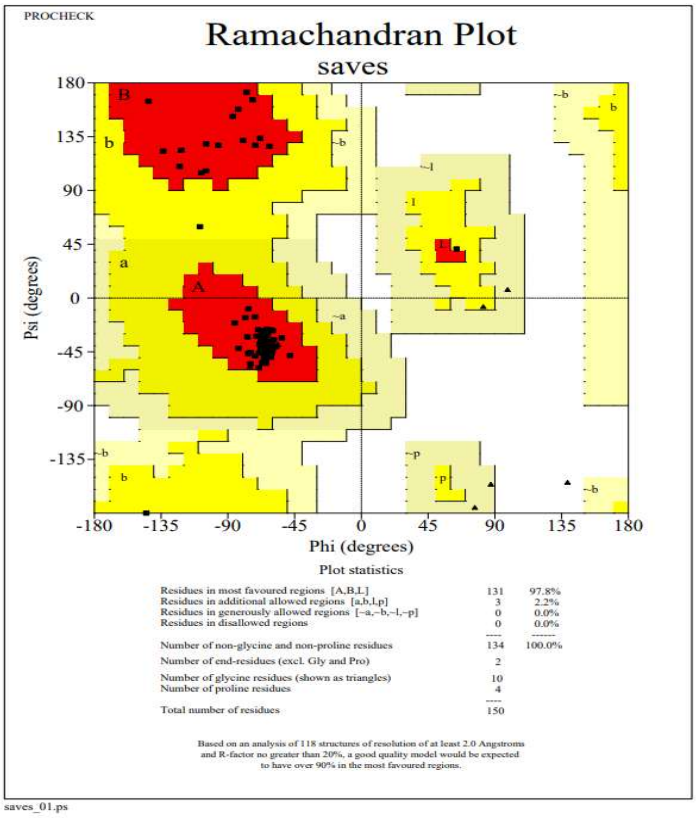

a

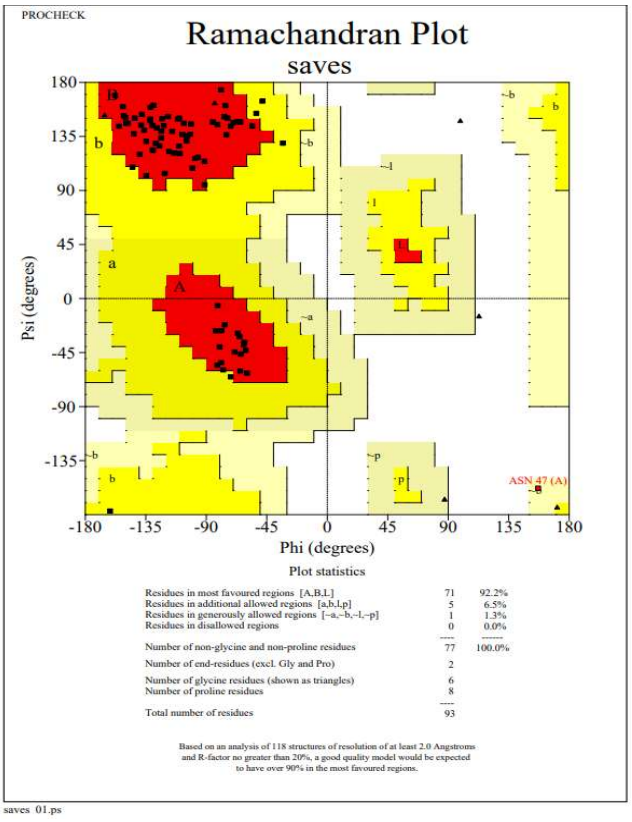

b

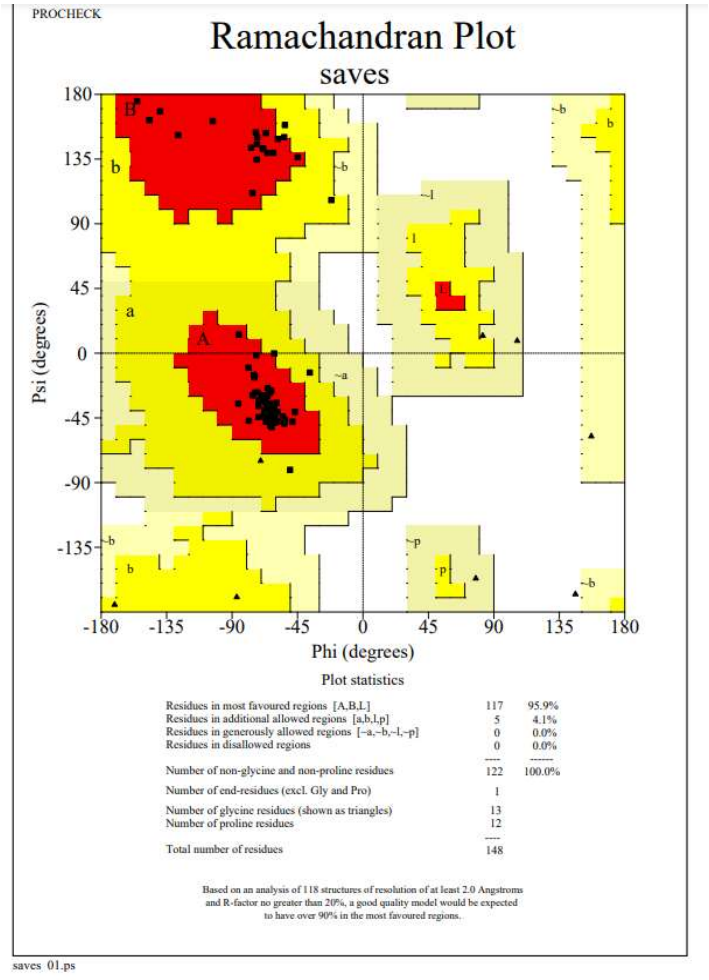

c

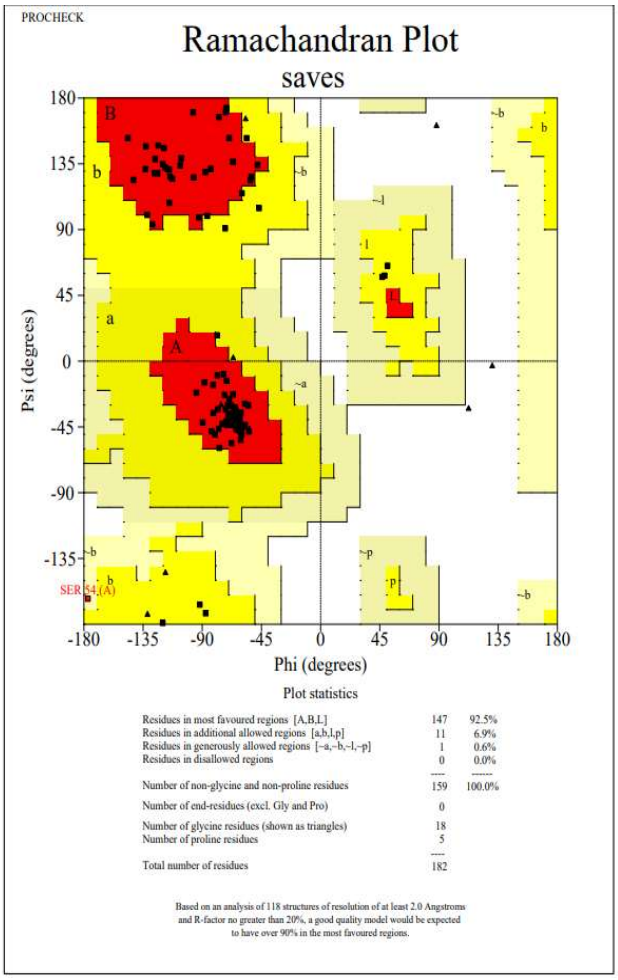

d

Figure 4(a),(b),(c),(d). Ramachandran Plots obtained from PROCHECK

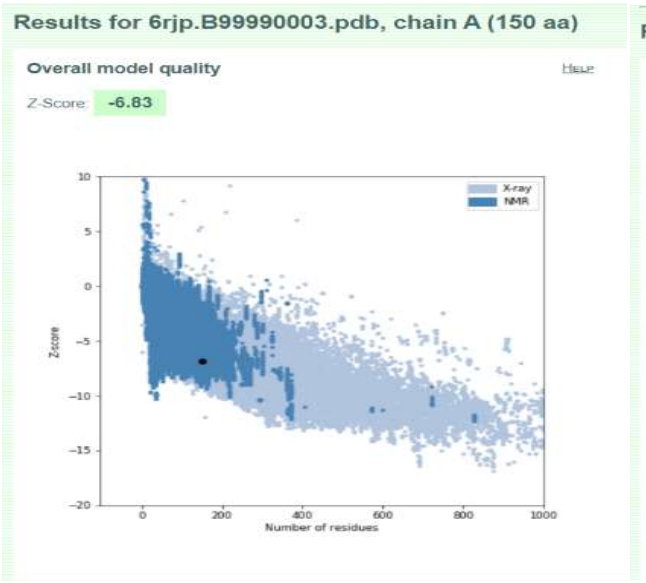

a

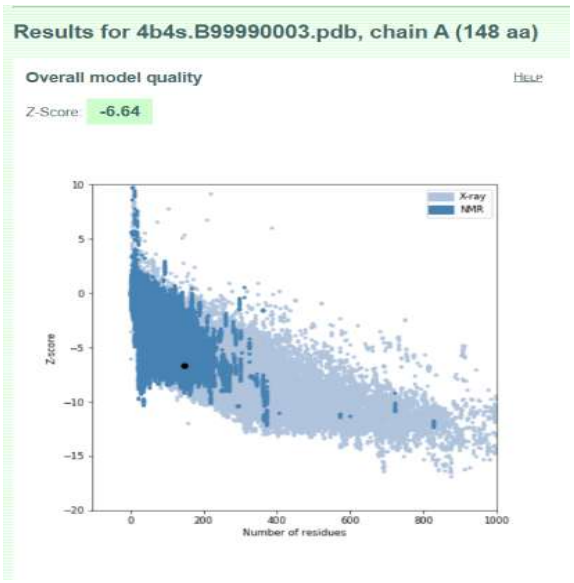

b

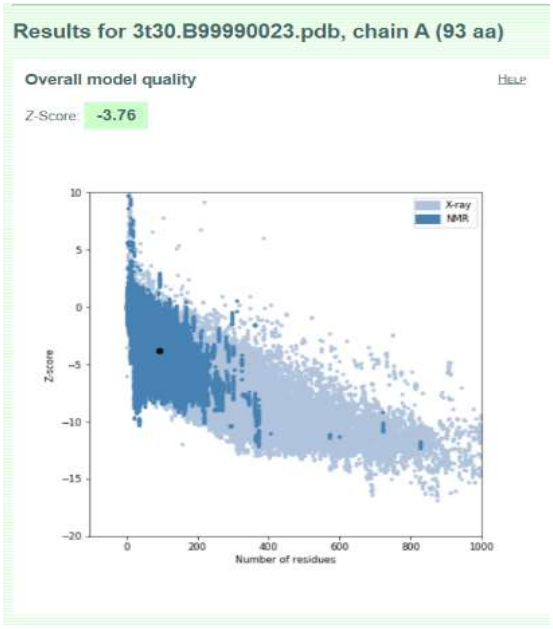

c

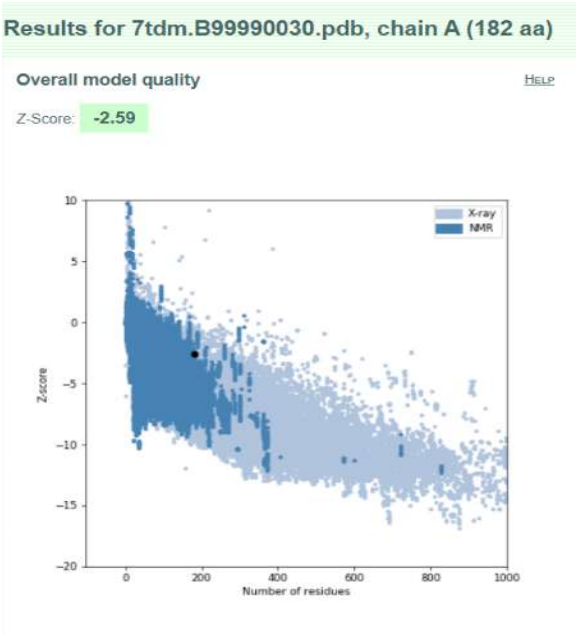

d

Figure 5(a),(b),(c),(d): Graphs obtained from ProSA showing overall model quality

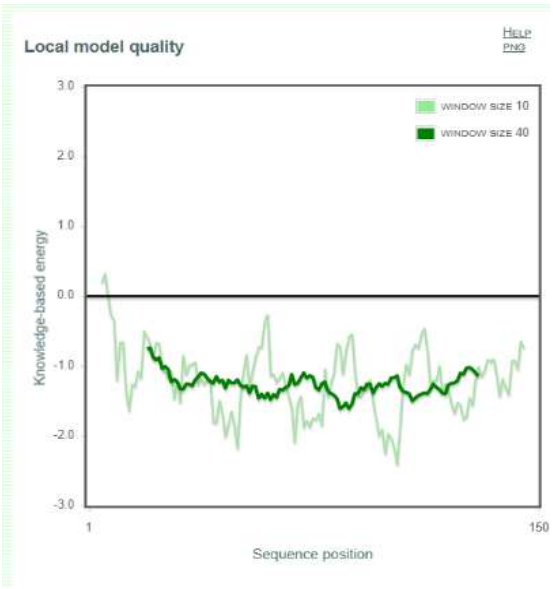

a

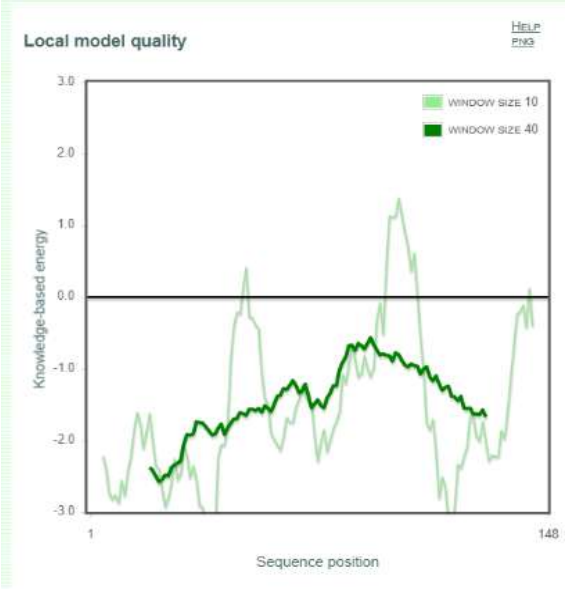

b

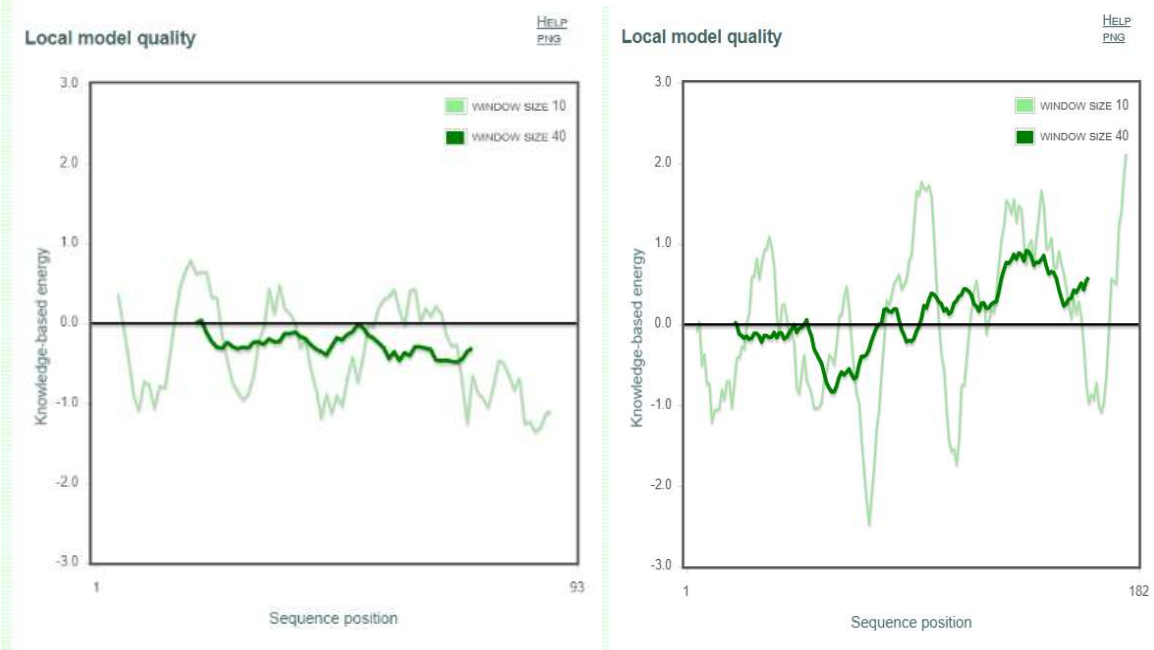

c d

Figure 6(a),(b),(c),(d): Graphs obtained from showing the local model quality

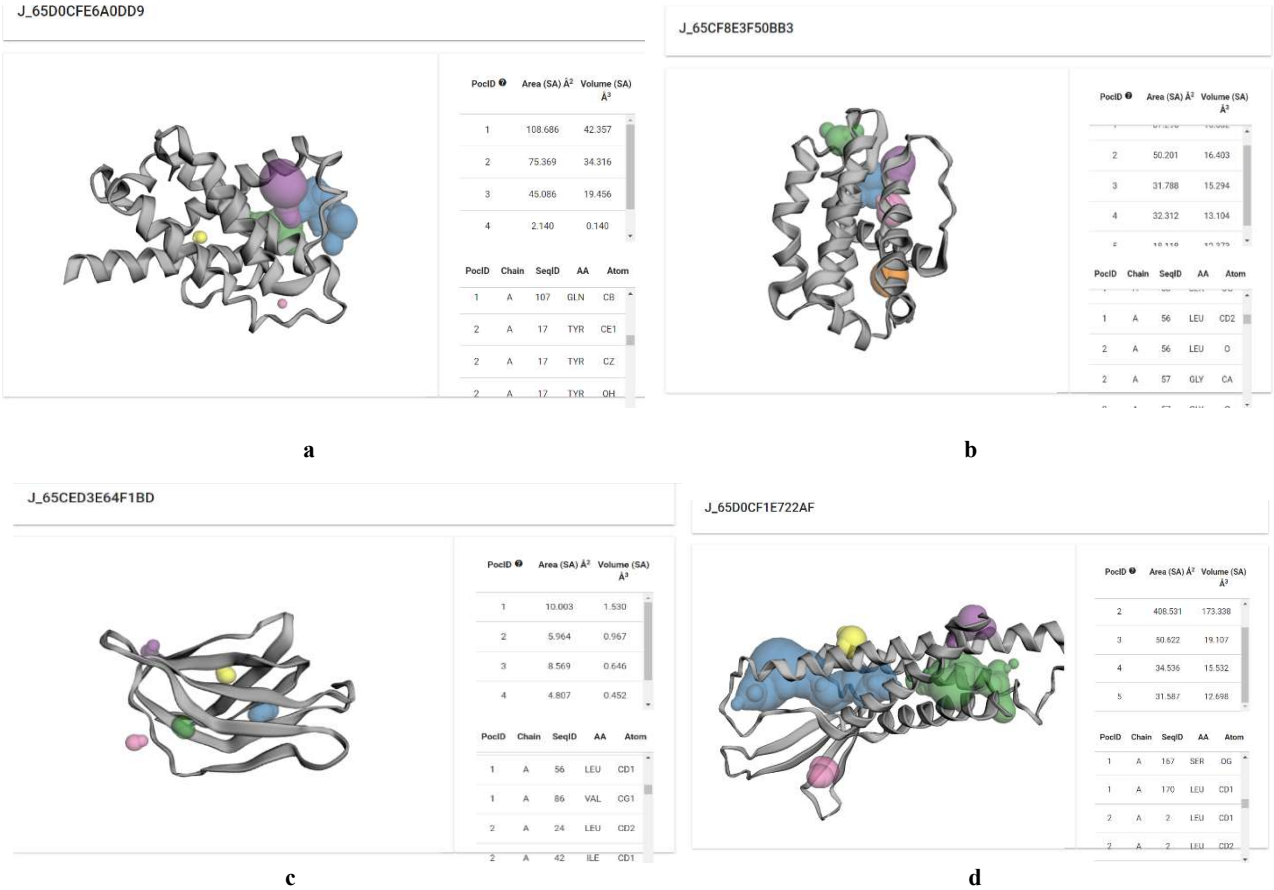

a **b**

c **d**

Figure 7(a),(b),(c),(d): Pockets and summary of volume and amino residues of the pockets

Binding affinity refers to the strength of the binding interaction between a protein and its ligand. A higher binding affinity indicates a weaker attraction and binding between the target molecule and ligand. Therefore, binding affinities should be negative, with lower values indicating better results.Hence, for each ligand, the conformation with the least affinity and 0 rmsd value is selected. Splitting of ligand files: This operation was performed using Vina software and Command Prompt.

AutoDockVina is a software that can be utilized to split the ligand files in their PDBQT format based on their rmsd values and binding affinities. The command prompt uses “vina_split” as a command to execute the process of splitting. Each ligand file is split into 10 conformations, which can be further analyzed to find the ligands with the binding affinities and rmsd values, and these are used as ligands in the final step for studying the ligand-protein interactions.

Visualisation of interactions between ligands and protein: The interactions between ligands and proteins are visualized using Discovery Studio in the form of 2D and 3D structures as given below.

Interaction of Alimta & Bevacizumab with Bcl-2-related protein A1

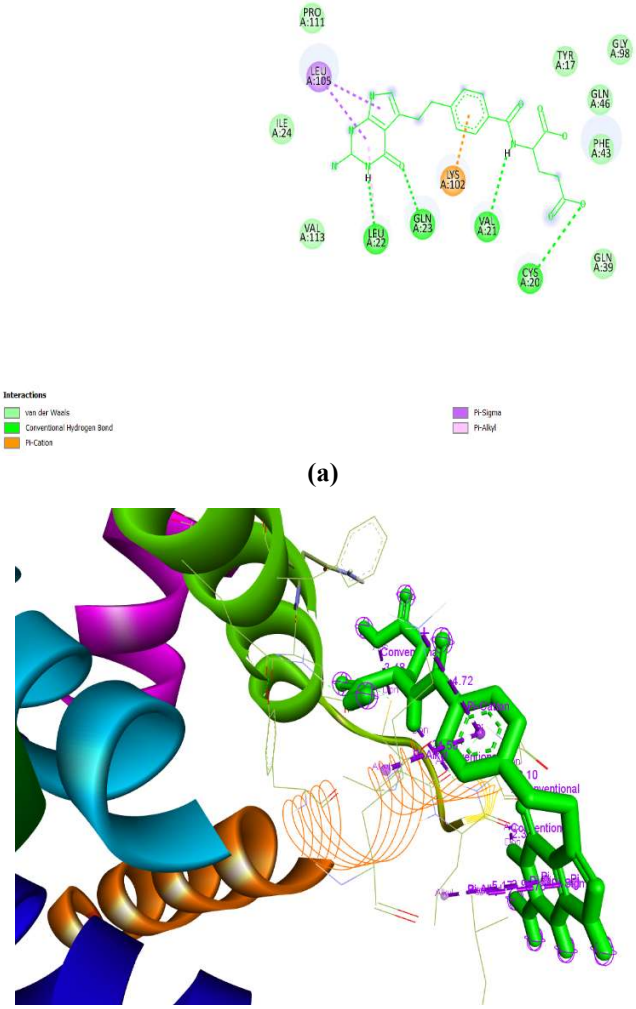

(a)

(b)

The interactions between the ligands i.e., the drugs and the protein were visualized in 2D and 3D form via Discovery Studio. 10 bonds were observed between Alimta and Bcl-2A1, 5 between Bevacizumab and Bcl-2A1.

Table 1. Summary of types of interactions between Alimta and Bcl-2-related protein A1

	NAME	DISTANCE	CATEGORY	TYPE	FROM	TO
2	A:CYS20:SG - :UNK0:O5	3.47899	Hydrogen Bond	Conventional Hydrogen Bond	A:CYS20:SG	:UNK0:O5
3	A:GLN23:HE21 - :UNK0:O1	2.09884	Hydrogen Bond	Conventional Hydrogen Bond	A:GLN23:HE21	:UNK0:O1
4	:UNK0:H48 - A:LEU22:O	2.35314	Hydrogen Bond	Conventional Hydrogen Bond	:UNK0:H48	A:LEU22:O
5	:UNK0:H43 - A:VAL21:O	2.72815	Hydrogen Bond	Conventional Hydrogen Bond	:UNK0:H43	A:VAL21:O
6	A:LYS102:NZ - :UNK0	4.72089	Electrostatic	Pi-Cation	A:LYS102:NZ	:UNK0
7	A:LEU105:CD2 - :UNK0	3.75991	Hydrophobic	Pi-Sigma	A:LEU105:CD2	:UNK0
8	A:LEU105:CD2 - :UNK0	3.96361	Hydrophobic	Pi-Sigma	A:LEU105:CD2	:UNK0
9	:UNK0 - A:LYS102	4.55338	Hydrophobic	Pi-Alkyl	:UNK0	A:LYS102
10	:UNK0 - A:LEU22	5.16996	Hydrophobic	Pi-Alkyl	:UNK0	A:LEU22

The ligand molecules exhibit the formation of Conventional Hydrogen bonds, Carbon-Hydrogen bonds, Pi-Alkyl bonds, Pi-sigma bonds, and bonds formed due to attractive charges with the amino acid residues LEU105, LEU22, GLN23, LYS102, VAL21, CYS20, PHE43, VAL21 of Bcl-2A1.

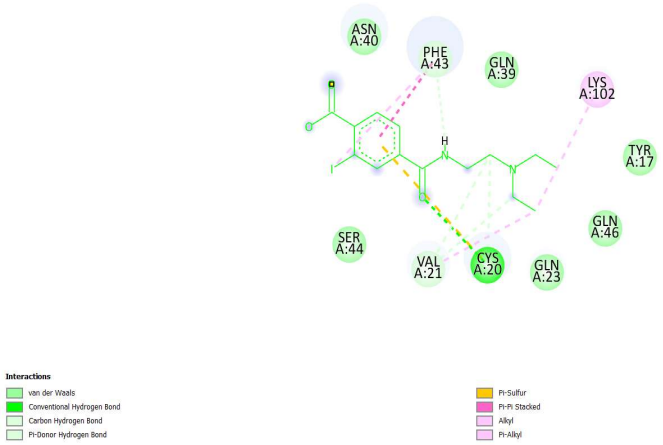

a

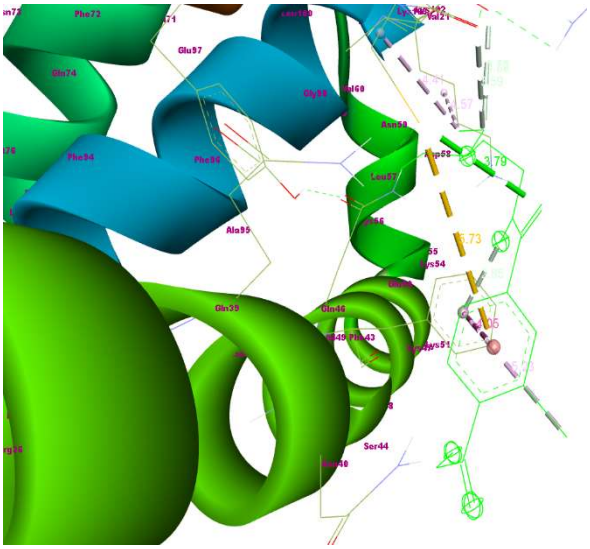

b

Figure 9. Docked pictures [(a) 2Dimensional (b) 3Dimensional] depicting the interactions between the virtual screened Bevacizumab and Bcl-2-related protein A1

Table 2. Summary of types of interactions between Bevacizumab and Bcl-2-related protein A1

	NAME	DISTANCE	CATEGORY	TYPE	FROM	TO
2	A:CYS20:SG - :UNK0:O2	3.79085	Hydrogen Bond	Conventional Hydrogen Bond	A:CYS20:SG	:UNK0:O2
3	:UNK0:C7 - A:CYS20:O	3.59408	Hydrogen Bond	Carbon Hydrogen Bond	:UNK0:C7	A:CYS20:O
4	:UNK0:C7 - A:VAL21:O	3.69486	Hydrogen Bond	Carbon Hydrogen Bond	:UNK0:C7	A:VAL21:O
5	:UNK0:C9 - A:VAL21:O	3.71694	Hydrogen Bond	Carbon Hydrogen Bond	:UNK0:C9	A:VAL21:O
6	:UNK0:H35 - A:PHE43					
7	A:CYS20:SG - :UNK0					
8	A:PHE43 - :UNK0					
9	:UNK0:C12 - A:VAL21					
10	:UNK0:C12 - A:LYS102					
11	A:PHE43 - :UNK0:I1					

Upon analysis of the types of bonds formed and the amino acids involved in bond formation (Table 4.6, 4.7), it was observed that the H-bond is formed predominantly by CYS20, VAL21, GLN23, and LEU22. It was also observed that most of the amino acids involved in bond formation belonged to pocket-2 and 3 (as seen in CASTp Table 4.1) indicating that the amino acid residues of pocket-2 and 3 can act

as good active sites for ligand binding and thus these amino acid residues could act as important sites for interaction of drugs with Bcl-2A1.

Interaction of Alimta & Bevacizumab with Bcl2-L-10-2

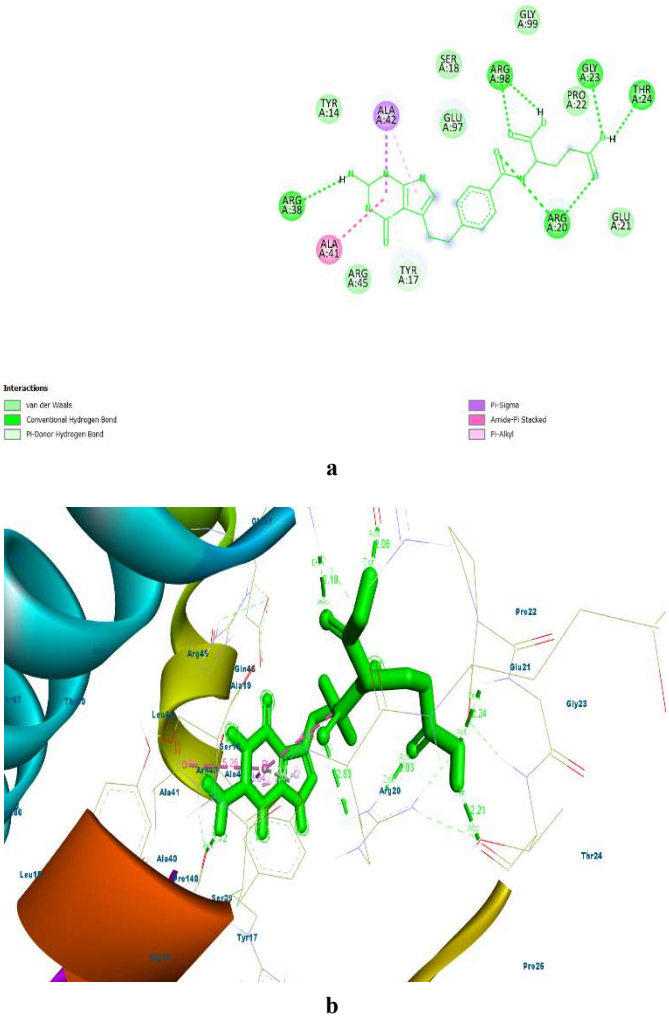

a

b

Figure 10. Docked pictures [(a) 2Dimensional (b) 3Dimensional] depicting the interactions between the virtual screened Alimta and Bcl-2-like protein isoform 2.

Table 3. Summary of types of interactions between Alimta and Bcl2-L-10-2

	NAME	DISTANCE	CATEGORY	TYPES	FROM	TO
2	A:ARG20:HH21 - :UNK0:O6	2.0347	Hydrogen Bond	Conventional Hydrogen Bond	A:ARG20:HH21	:UNK0:O6
3	A:ARG20:HH22 - :UNK0:O2	2.8317	Hydrogen Bond	Conventional Hydrogen Bond	A:ARG20:HH22	:UNK0:O2
4	A:GLY23:HN - :UNK0:O5	2.24289	Hydrogen Bond	Conventional Hydrogen Bond	A:GLY23:HN	:UNK0:O5
5	A:ARG98:HN - :UNK0:O4	2.1896	Hydrogen Bond	Conventional Hydrogen Bond	A:ARG98:HN	:UNK0:O4
6	:UNK0:H49 - A:ARG38:O	2.7163	Hydrogen Bond	Conventional Hydrogen Bond	:UNK0:H49	A:ARG38:O
7	:UNK0:H52 - A:THR24:O	2.20845	Hydrogen Bond	Conventional Hydrogen Bond	:UNK0:H52	A:THR24:O
8	:UNK0:H51 - A:ARG98:O	2.06202	Hydrogen Bond	Conventional Hydrogen Bond	:UNK0:H51	A:ARG98:O
9	A:TYR17:HH - :UNK0	3.0656	Hydrogen Bond	Pi-Donor Hydrogen Bond	A:TYR17:HH	:UNK0
10	A:ALA42:CB - :UNK0	3.6437	Hydrophobic	Pi-Sigma	A:ALA42:CB	:UNK0
11	:UNK0 - :UNK0	4.80732	Hydrophobic	Pi-Pi T-shaped	:UNK0	:UNK0
12	A:ALA41:C,O;ALA42:N - :UNK0	5.2622	Hydrophobic	Amide-Pi Stacked	A:ALA41:C,O;ALA42:N	:UNK0
13	:UNK0 - A:ALA42	4.16274	Hydrophobic	Pi-Alkyl	:UNK0	A:ALA42

The interactions between the ligands, i.e., the drugs and the protein, were visualized in 2D and 3D form via Discovery Studio. 13 bonds were observed between Alimta and Bcl2-L-10-2, 10 between Bevacizumab and Bcl2-L-10-2.

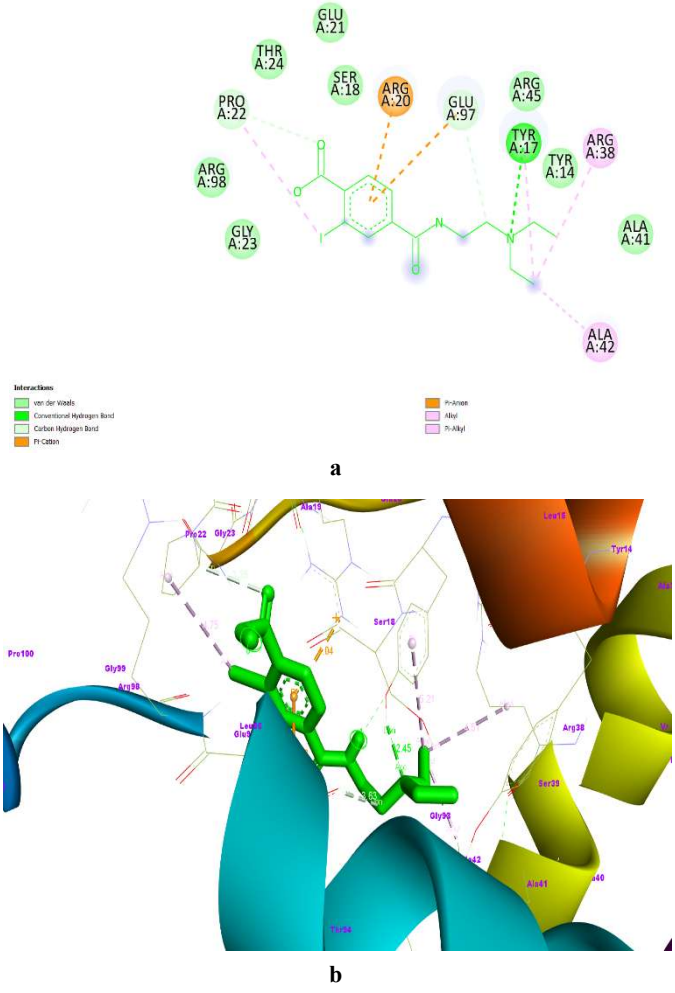

a

b

Figure 11. Docked pictures [(a) 2Dimensional (b) 3Dimensional] depicting the interactions between the virtual screened Alimta and Bcl-2-like protein isoform 2

Table 4. Summary of types of interactions between Bevacizumab and Bcl2-L-10-2

	NAME	DISTANCE	CATEGORY	TYPES	FROM	TO
2	A:TYR17:HH - :UNK0:N5	2.44779	Hydrogen Bond	Conventional Hydrogen Bond	A:TYR17:HH	:UNK0:N5
3	A:PRO22:CA - :UNK0:O4	3.35202	Hydrogen Bond	Carbon Hydrogen Bond	A:PRO22:CA	:UNK0:O4
4	:UNK0:C7 - A:GLU97:OE2	3.62852	Hydrogen Bond	Carbon Hydrogen Bond	:UNK0:C7	A:GLU97:OE2
5	A:ARG20:NH2 - :UNK0	4.04138	Electrostatic	Pi-Cation	A:ARG20:NH2	:UNK0
6	A:GLU97:OE1 - :UNK0	4.7834	Electrostatic	Pi-Anion	A:GLU97:OE1	:UNK0
7	A:ALA42 - :UNK0:C12	4.06724	Hydrophobic	Alkyl	A:ALA42	:UNK0:C12
8	:UNK0:I1 - A:PRO22	4.7487	Hydrophobic	Alkyl	:UNK0:I1	A:PRO22
9	:UNK0:C12 - A:ARG38	4.51453	Hydrophobic	Alkyl	:UNK0:C12	A:ARG38
10	A:TYR17 - :UNK0:C12	5.20833	Hydrophobic	Pi-Alkyl	A:TYR17	:UNK0:C12

The ligand molecules exhibit the formation of Conventional Hydrogen bonds, Carbon-Hydrogen bonds, Pi-Donor Hydrogen bonds, Pi-Pi T-shaped bonds, Amide-Pi stacked bonds, Pi-Alkyl bonds, Pi-sigma bonds, Pi-Cation, Pi-Anion and Alkyl bonds with the amino acid residues ARG38, ALA42, ALA41, ARG98, ARG20, GLY23, THRI24, PRO22, GLU97, TYR17of Bcl2-L-10-2.Upon analysis of the types of bonds formed and the amino acids involved in bond formation (Table 4.8, 4.9), it was observed that the H-bond is formed predominantly by ARG38, ARG20, ARG98, GLY23, THRI24, and TYR17.It was also observed that most of the amino acids involved in bond formation belonged to pocket-2 (as seen in CASTp Table 4.2) indicating that the amino acid residues of pocket-2 can act as good active sites for ligand binding. Thus, these amino acid

residues could act as important sites for the interaction of drugs with Bcl2-L-10-2.

Interaction of Alimta & Bevacizumab with NPM2

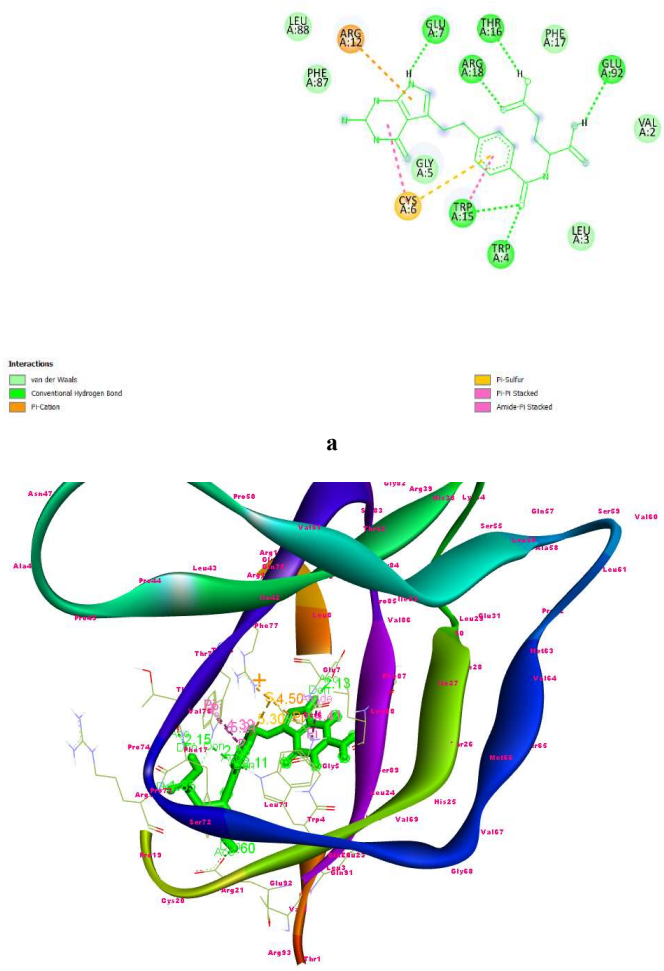

Figure 12. Docked pictures [(a) 2Dimensional (b) 3Dimensional] depicting the interactions between the virtual screened Alimta and NPM2

Table 5. Summary of types of interactions between Alimta and NPM2

	NAME	DISTANCE	CATEGORY	TYPE	FROM	TO
2	A:TRP4:HE1 - :UNK0:O2	2.10903	Hydrogen Bond	Conventional Hydrogen Bond	A:TRP4:HE1	:UNK0:O2
3	A:TRP15:HE1 - :UNK0:O2	2.53101	Hydrogen Bond	Conventional Hydrogen Bond	A:TRP15:HE1	:UNK0:O2
4	A:ARG18:HN - :UNK0:O6	1.8528	Hydrogen Bond	Conventional Hydrogen Bond	A:ARG18:HN	:UNK0:O6
5	:UNK0:H40 - A:GLU7:OE1	2.13443	Hydrogen Bond	Conventional Hydrogen Bond	:UNK0:H40	A:GLU7:OE1
6	:UNK0:H52 - A:THR16:O	2.1548	Hydrogen Bond	Conventional Hydrogen Bond	:UNK0:H52	A:THR16:O
7	:UNK0:H51 - A:GLU92:OE1	2.59921	Hydrogen Bond	Conventional Hydrogen Bond	:UNK0:H51	A:GLU92:OE1
8	A:ARG12:NH1 - :UNK0	4.49846	Electrostatic	Pi-Cation	A:ARG12:NH1	:UNK0
9	A:CYS6:SG - :UNK0	5.30157	Other	Pi-Sulfur	A:CYS6:SG	:UNK0
10	A:TRP15 - :UNK0	5.20586	Hydrophobic	Pi-Pi Stacked	A:TRP15	:UNK0
11	A:TRP15 - :UNK0	4.32003	Hydrophobic	Pi-Pi Stacked	A:TRP15	:UNK0
12	A:CYS6:C,O;GLU7:N - :UNK0	4.41003	Hydrophobic	Amide-Pi Stacked	A:CYS6:C,O;GLU7:N	:UNK0

The interactions between the ligands, i.e., the drugs and the protein, were visualized in 2D and 3D form via Discovery Studio. 12 bonds were observed between Alimta and NPM2, 7 between Bevacizumab and NPM2. The ligand molecules exhibit the formation of Conventional Hydrogen bonds, Carbon-Hydrogen bonds, Pi-Pi Stacked bonds, Pi-Sulfur bonds, Amide-Pi stacked bonds, Pi-Alkyl bonds, and Pi-Cation with the amino acid residues ARG12, ARG18, GLU7, THR16, CYS6, TRP15, TRP4, GLU92, GLU31, GLY30, LYS32, PHE87, LEU88 of NPM2.

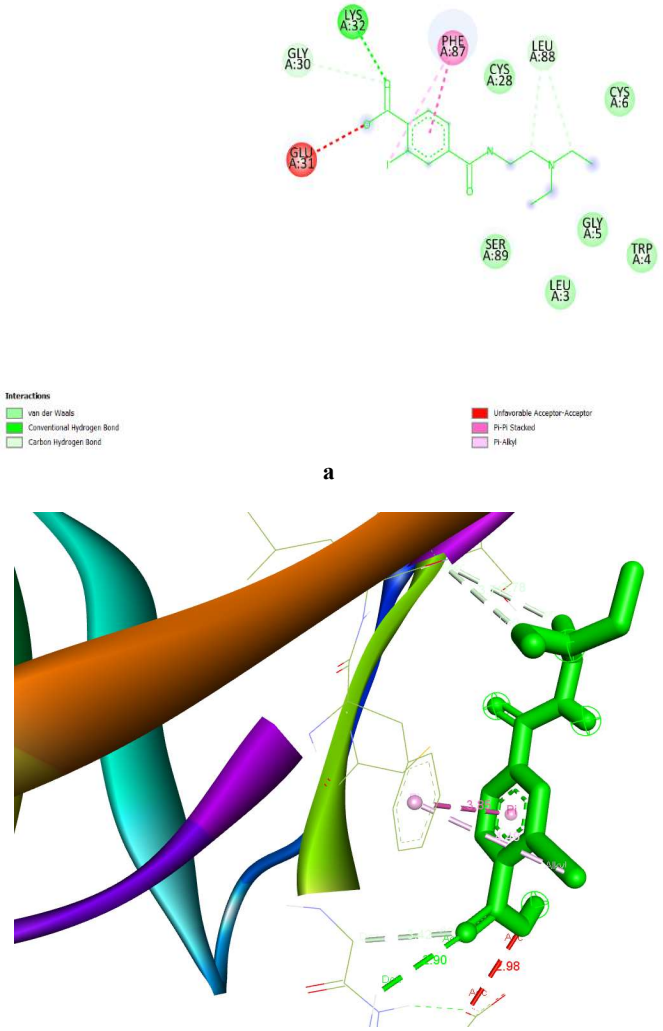

Figure 13. Docked pictures [(a) 2Dimensional (b) 3Dimensional] depicting the interactions between the virtual screened Bevacizumab and NPM2

Table 6. Summary of types of interactions between Bevacizumab and NPM2

	NAME	DISTANCE	CATEGORY	TYPE	FROM	TO
2	A:LYS32:HZ1 - :UNK0:O4	2.9018	Hydrogen Bond	Conventional Hydrogen Bond	A:LYS32:HZ1	:UNK0:O4
3	A:GLY30:CA - :UNK0:O4	3.41958	Hydrogen Bond	Carbon Hydrogen Bond	A:GLY30:CA	:UNK0:O4
4	:UNK0:C7 - A:LEU88:O	3.78443	Hydrogen Bond	Carbon Hydrogen Bond	:UNK0:C7	A:LEU88:O
5	:UNK0:C9 - A:LEU88:O	3.70551	Hydrogen Bond	Carbon Hydrogen Bond	:UNK0:C9	A:LEU88:O
6	A:PHE87 - :UNK0	3.84643	Hydrophobic	Pi-Pi Stacked	A:PHE87	:UNK0
7	A:PHE87 - :UNK0:I1	4.49323	Hydrophobic	Pi-Alkyl	A:PHE87	:UNK0:I1

Upon analysis of the types of bonds formed and the amino acids involved in bond formation (Table 4.10, 4.11), it was observed the H-bond is formed predominantly by GLU7, ARG18, THR16, GLU92, TRP4, TRP15, and LYS32.

It was also observed that most of the amino acids involved in bond formation belonged to pocket-4 (as seen in CASTp Table 4.3) indicating that the amino acid residues of pocket-4 can act as good active sites for ligand binding and thus these amino acid residues could act as important sites for interaction of drugs with NPM2.

Interaction of Alimta & Bevacizumab with CLDN-4

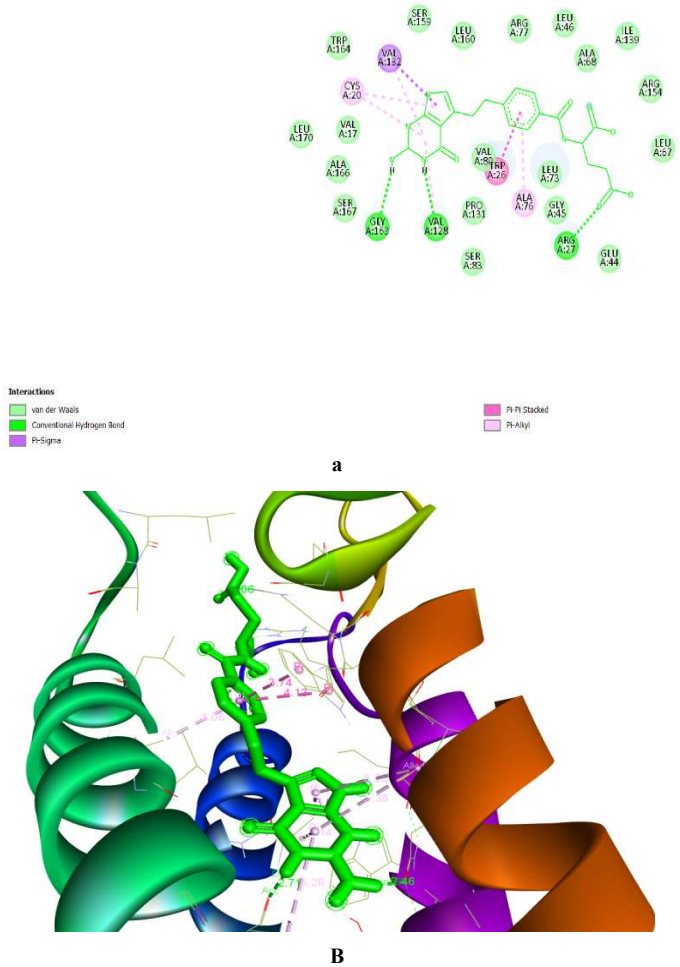

Figure 14. Docked pictures [(a) 2Dimensional (b) 3Dimensional] depicting the interactions between the virtually screened Alimta and CLDN-4

Table 7. Summary of types of interactions between Alimta and CLDN-4

	NAME	DISTANCE	CATEGORY	TYPE	FROM	TO
2	A:ARG27:HH12 - :UNK0:O6	2.0612	Hydrogen Bond	Conventional Hydrogen Bond	A:ARG27:HH12	:UNK0:O6
3	:UNK0:H48 - A:VAL128:O	2.70965	Hydrogen Bond	Conventional Hydrogen Bond	:UNK0:H48	A:VAL128:O
4	:UNK0:H49 - A:GLY163:O	2.45503	Hydrogen Bond	Conventional Hydrogen Bond	:UNK0:H49	A:GLY163:O
5	A:VAL132:CG2 - :UNK0	3.6217	Hydrophobic	Pi-Sigma	A:VAL132:CG2	:UNK0
6	A:TRP26 - :UNK0	4.12595	Hydrophobic	Pi-Pi Stacked	A:TRP26	:UNK0
7	A:TRP26 - :UNK0	3.73708	Hydrophobic	Pi-Pi Stacked	A:TRP26	:UNK0
8	:UNK0 - A:ALA76	4.08004	Hydrophobic	Pi-Alkyl	:UNK0	A:ALA76
9	:UNK0 - A:CYS20	5.21619	Hydrophobic	Pi-Alkyl	:UNK0	A:CYS20
10	:UNK0 - A:CYS20	5.36451	Hydrophobic	Pi-Alkyl	:UNK0	A:CYS20
11	:UNK0 - A:VAL128	5.27913	Hydrophobic	Pi-Alkyl	:UNK0	A:VAL128
12	:UNK0 - A:VAL132	4.14423	Hydrophobic	Pi-Alkyl	:UNK0	A:VAL132

The interactions between the ligands, i.e., the drugs and the protein, were visualized in 2D and 3D form via Discovery Studio. 12 bonds were observed between Alimta and CLDN-4, 8 between Bevacizumab and CLDN-4. The ligand molecules exhibit the formation of Conventional Hydrogen bonds, Pi-sigma bonds, Pi-Pi Stacked bonds, Pi-Alkyl bonds, and Alkyl bonds with the amino acid residues VAL132, CYS20, GLY163, VAL128, TRP26, ALA76, ARG27, LEU73, VAL80 of CLDN-4. Upon analysis of the types of bonds formed and the amino acids involved in bond formation (Table 4.12, 4.13), it was observed that the H-bond is formed predominantly by GLY163, VAL128, ARG27, and LEU73.

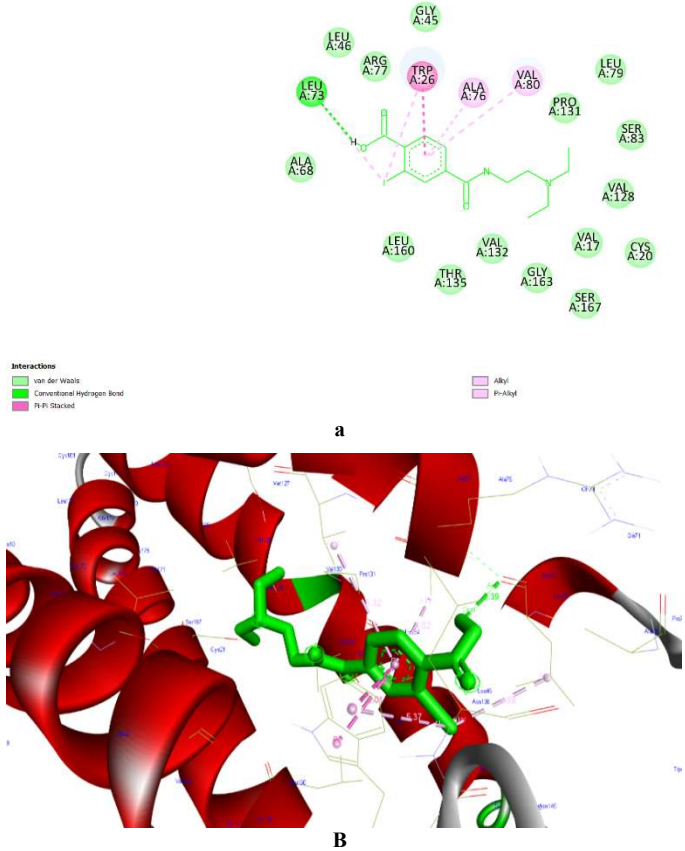

Figure 15. Docked pictures [(a) 2Dimensional (b) 3Dimensional] depicting the interactions between the virtually screened Bevacizumab and CLDN-4

Table 8. Summary of types of interactions between Bevacizumab and CLDN-4

	NAME	DISTANCE	CATEGORY	TYPES	FROM	TO
2	:UNK0:H39 - A:LEU73:O	2.39304	Hydrogen Bond	Conventional Hydrogen Bond	:UNK0:H39	A:LEU73:O
3	A:TRP26 - :UNK0	4.01155	Hydrophobic	Pi-Pi Stacked	A:TRP26	:UNK0
4	A:TRP26 - :UNK0	3.66645	Hydrophobic	Pi-Pi Stacked	A:TRP26	:UNK0
5	:UNK0:I1 - A:LEU73	4.68403	Hydrophobic	Alkyl	:UNK0:I1	A:LEU73
6	A:TRP26 - :UNK0:I1	5.37068	Hydrophobic	Pi-Alkyl	A:TRP26	:UNK0:I1
7	:UNK0 - A:ALA76	4.01627	Hydrophobic	Pi-Alkyl	:UNK0	A:ALA76
8	:UNK0 - A:VAL80	5.3195	Hydrophobic	Pi-Alkyl	:UNK0	A:VAL80

It was also observed that most of the amino acids involved in bond formation belonged to pocket-1,2,3 & 4 (as seen in CASTp Table 4.4) indicating that the amino acid residues of pocket-1,2,3 & 4 can act as good active sites for ligand binding and thus these amino acid residues could act as important sites for interaction of drugs with CLDN-4.

CONCLUSION

Mesothelioma, a cancer affecting the mesothelium lining various internal organs, presents a grim prognosis with a typical survival rate of 4 to 18 months post-diagnosis and a five-year survival rate of just 10 percent. Over the years, mesothelioma cases have surged by more than 36%, underscoring the urgent need for novel treatment options. Current therapies often fall short in managing advanced cases, leading to low survival probability and compromised quality of life for patients. Addressing this pressing global health challenge requires innovative drug development efforts. One promising avenue lies in personalized medicine, offering tailored interventions for mesothelioma patients. However, collaborative research endeavours are essential to bring accessible and effective drugs to fruition. Leveraging bioinformatics tools for in silico drug design presents a faster and more efficient alternative to traditional laboratory methods.

In the above context, this study is focused on elucidating the interactions between key proteins implicated in mesothelioma—such as Claudin-4, Bcl-2-related protein A1, nucleoplasmin-2 isoform 2, and bcl-2-like protein 10 isoform 2—and established mesothelioma drugs like Alimta and Bevacizumab. Utilizing homology modeling, we generated 3D structures of these proteins and conducted docking studies to identify critical binding residues. The findings highlight specific amino acid residues within these proteins—such as LEU105, LEU22, GLN23, LYS102, VAL21, CYS20, PHE43, and VAL21 in *Bcl-2A1*; ARG38, ALA42, ALA41, ARG98, ARG20, GLY23, THR124, PRO22, GLU97, and TYR17 in *Bcl2-L-10-2*; ARG12, ARG18, GLU7, THR16, CYS6, TRP15, TRP4, GLU92, GLU31, GLY30, LYS32, PHE87, and LEU88 in *NPM2*; and VAL132, CYS20, GLY163, VAL128, TRP26, ALA76, ARG27, LEU73, and VAL80 in *CLDN-4* as crucial for drug binding and potential inhibition of mesothelioma cell replication. By targeting these key residues, novel drugs may effectively disrupt mesothelioma progression, offering hope for improved patient outcomes.

REFERENCES

Arulananda, S., Lee, E. F., Fairlie, W. D., & John, T. 2021. The role of BCL-2 family proteins and therapeutic potential of BH3-mimetics in malignant pleural mesothelioma. *Expert Review of Anticancer Therapy*, *21*(4), 413–424. https://doi.org/10.1080/14737140.2021.1856660

Facchetti, F., Lonardi, S., Gentili, F., Bercich, L., Falchetti, M., Tardanico, R., Baronchelli, C., Lucini, L., Santin, A., & Murer, B. (2007). Claudin 4 identifies a wide spectrum of epithelial neoplasms and represents a very useful marker for carcinoma versus mesothelioma diagnosis in pleural and peritoneal biopsies and effusions. *VirchowsArchiv*, *451*(3), 669–680. https://doi.org/10.1007/s00428-007-0448-x

Fujiwara-Tani, R., Mori, S., Ogata, R., Sasaki, R., Ikemoto, A., Kishi, S., Kondoh, M., &Kuniyasu, H. (2023). Claudin-4: A New Molecular Target for Epithelial Cancer Therapy. *International Journal of Molecular Sciences*, *24*(6), 5494. https://doi.org/10.3390/ijms24065494

Gardner, C. R. (2004). Anticancer drug development based on modulation of the Bcl-2 family core apoptosis mechanism. *Expert Review of Anticancer Therapy*, *4*(6), 1157–1177. https://doi.org/10.1586/14737140.4.6.1157

Green, M. R. (2002). Alimta (pemetrexed disodium): A multitargeted antifolate for the treatment of mesothelioma. *Lung Cancer*, *38*, 55–57. https://doi.org/10.1016/S0169-5002(02)00359-8

Jackson, M. R., Ashton, M., Koessinger, A. L., Dick, C., Verheij, M., & Chalmers, A. J. (2020). Mesothelioma Cells Depend on the Antiapoptotic Protein Bcl-xL for Survival and Are Sensitized to Ionizing Radiation by BH3-Mimetics. *International Journal of Radiation Oncology*Biology*Physics*, *106*(4), 867–877. https://doi.org/10.1016/j.ijrobp.2019.11.029

Jean, D., &Jaurand, M.-C. (2015). Causes and pathophysiology of malignant pleural mesothelioma. *Lung Cancer Management*, *4*(5), 219–229. https://doi.org/10.2217/lmt.15.21

Kannerstein, M., & Churg, J. (1977). Peritoneal mesothelioma. *Human Pathology*, *8*(1), 83–94. https://doi.org/10.1016/S0046-8177(77)80067-1

Kirkin, V., Joos, S., &Zörnig, M. (2004a). The role of Bcl-2 family members in tumorigenesis. *Biochimica et Biophysica Acta (BBA) -Molecular Cell Research*, *1644*(2), 229–249. https://doi.org/10.1016/j.bbamcr.2003.08.009

Kirkin, V., Joos, S., &Zörnig, M. (2004b). The role of Bcl-2 family members in tumorigenesis. *Biochimica et Biophysica Acta (BBA) - Molecular Cell Research*, *1644*(2), 229–249. https://doi.org/10.1016/j.bbamcr.2003.08.009

Maji, S., Panda, S., Samal, S. K., Shriwas, O., Rath, R., Pellecchia, M., Emdad, L., Das, S. K., Fisher, P. B., & Dash, R. (2018a). Chapter Three—Bcl-2 Antiapoptotic Family Proteins and Chemoresistance in Cancer. In K. D. Tew & P. B. Fisher (Eds.), *Advances in Cancer Research* (Vol. 137, pp. 37–75). Academic Press. https://doi.org/10.1016/bs.acr.2017.11.001

Maji, S., Panda, S., Samal, S. K., Shriwas, O., Rath, R., Pellecchia, M., Emdad, L., Das, S. K., Fisher, P. B., & Dash, R. (2018b). Chapter Three—Bcl-2 Antiapoptotic Family Proteins and Chemoresistance in Cancer. In K. D. Tew & P. B. Fisher (Eds.), *Advances in Cancer Research* (Vol. 137, pp. 37–75). Academic Press. https://doi.org/10.1016/bs.acr.2017.11.001

Martini, N., McCormack, P. M., Bains, M. S., Kaiser, L. R., Burt, M. E., &Hilaris, B. S. (1987). Pleural Mesothelioma. *The Annals of Thoracic Surgery*, *43*(1), 113–120. https://doi.org/10.1016/S0003-4975(10)60182-8

McDonald, J. C., & McDonald, A. D. (1996). The epidemiology of mesothelioma in historical context. *European Respiratory Journal*, *9*(9), 1932–1942. https://doi.org/10.1183/09031936.96.09091932

Naso, J. R., & Churg, A. (2020). Claudin-4 shows superior specificity for mesothelioma vs non–small-cell lung carcinoma compared with MOC-31 and Ber-EP4. *Human Pathology*, *100*, 10–14. https://doi.org/10.1016/j.humpath.2020.04.005

Novel insights into mesothelioma biology and implications for therapy | Nature Reviews Cancer. (n.d.). Retrieved 29 February 2024, from https://www.nature.com/articles/nrc.2017.42

O'Kane, S. L., Pound, R. J., Campbell, A., Chaudhuri, N., Lind, M. J., & Cawkwell, L. (2006). Expression of bcl-2 family members in malignant pleural mesothelioma. *Acta Oncologica (Stockholm, Sweden)*, *45*(4), 449–453. https://doi.org/10.1080/02841860500468927

Pathology of malignant mesothelioma—ATTANOOS - 1997—Histopathology—Wiley Online Library. (n.d.). Retrieved 29 February 2024, from https://onlinelibrary.wiley.com/doi/abs/10.1046/j.1365-2559.1997.5460776.x

Predicting the accuracy of protein–ligand docking on homology models—Bordogna—2011—Journal of Computational Chemistry—Wiley Online Library. (n.d.). Retrieved 29 February 2024, from https://onlinelibrary.wiley.com/doi/abs/10.1002/jcc.21601

Proteomics in Functional Genomics: Protein Structure Analysis | SpringerLink. (n.d.). Retrieved 29 February 2024, from https://link.springer.com/book/10.1007/978-3-0348-8458-7#page=220

Robinson, B. W., Musk, A. W., & Lake, R. A. (2005). Malignant mesothelioma. *The Lancet*, *366*(9483), 397–408. https://doi.org/10.1016/S0140-6736(05)67025-0

The BCL-2 protein family: Opposing activities that mediate cell death | Nature Reviews Molecular Cell Biology. (n.d.). Retrieved 29 February 2024, from https://www.nature.com/articles/nrm2308

Wu, H., Yang, Z., Yan, L., Su, Y., Ma, R., & Li, Y. (2022). NPM2 in malignant peritoneal mesothelioma: From basic tumor biology to clinical medicine. *World Journal of Surgical Oncology*, *20*, 141. https://doi.org/10.1186/s12957-022-02604-3

Youle, R. J., & Strasser, A. (2008). The BCL-2 protein family: Opposing activities that mediate cell death. *Nature Reviews Molecular Cell Biology*, *9*(1), Article 1. https://doi.org/10.1038/nrm2308

Zalcman, G., Mazieres, J., Margery, J., Greillier, L., Audigier-Valette, C., Moro-Sibilot, D., Molinier, O., Corre, R., Monnet, I., Gounant, V., Rivière, F., Janicot, H., Gervais, R., Locher, C., Milleron, B., Tran, Q., Lebitasy, M.-P., Morin, F., Creveuil, C., … Scherpereel, A. (2016). Bevacizumab for newly diagnosed pleural mesothelioma in the Mesothelioma Avastin Cisplatin Pemetrexed Study (MAPS): A randomised, controlled, open-label, phase 3 trial. *The Lancet*, *387*(10026), 1405–1414. https://doi.org/10.1016/S0140-6736(15)01238-6

Zhang, H., Holzgreve, W., & De Geyter, C. (2001a). Bcl2-L-10, a novel anti-apoptotic member of the Bcl-2 family, blocks apoptosis in the mitochondria death pathway but not in the death receptor pathway. *Human Molecular Genetics*, *10*(21), 2329–2339. https://doi.org/10.1093/hmg/10.21.2329

Zhang, H., Holzgreve, W., & De Geyter, C. (2001b). Bcl2-L-10, a novel anti-apoptotic member of the Bcl-2 family, blocks apoptosis in the mitochondria death pathway but not in the death receptor pathway. *Human Molecular Genetics*, *10*(21), 2329–2339. https://doi.org/10.1093/hmg/10.21.2329

****